Supplementary Materials

LCAT-Remodeled Structural Transition of Reconstituted HDL Enhances SR-BI Binding

Ying Wang, Xiaoyu Sun, Wentong He, Yi Ding, and Wen Chen *

College of Food Science and Technology, South China University of Technology, Guangzhou 510000, China
* Correspondence: wenchen@scut.edu.cn
Received: 14 April 2026; Revised: 2 June 2026; Accepted: 9 June 2026; Published: 15 October 2026

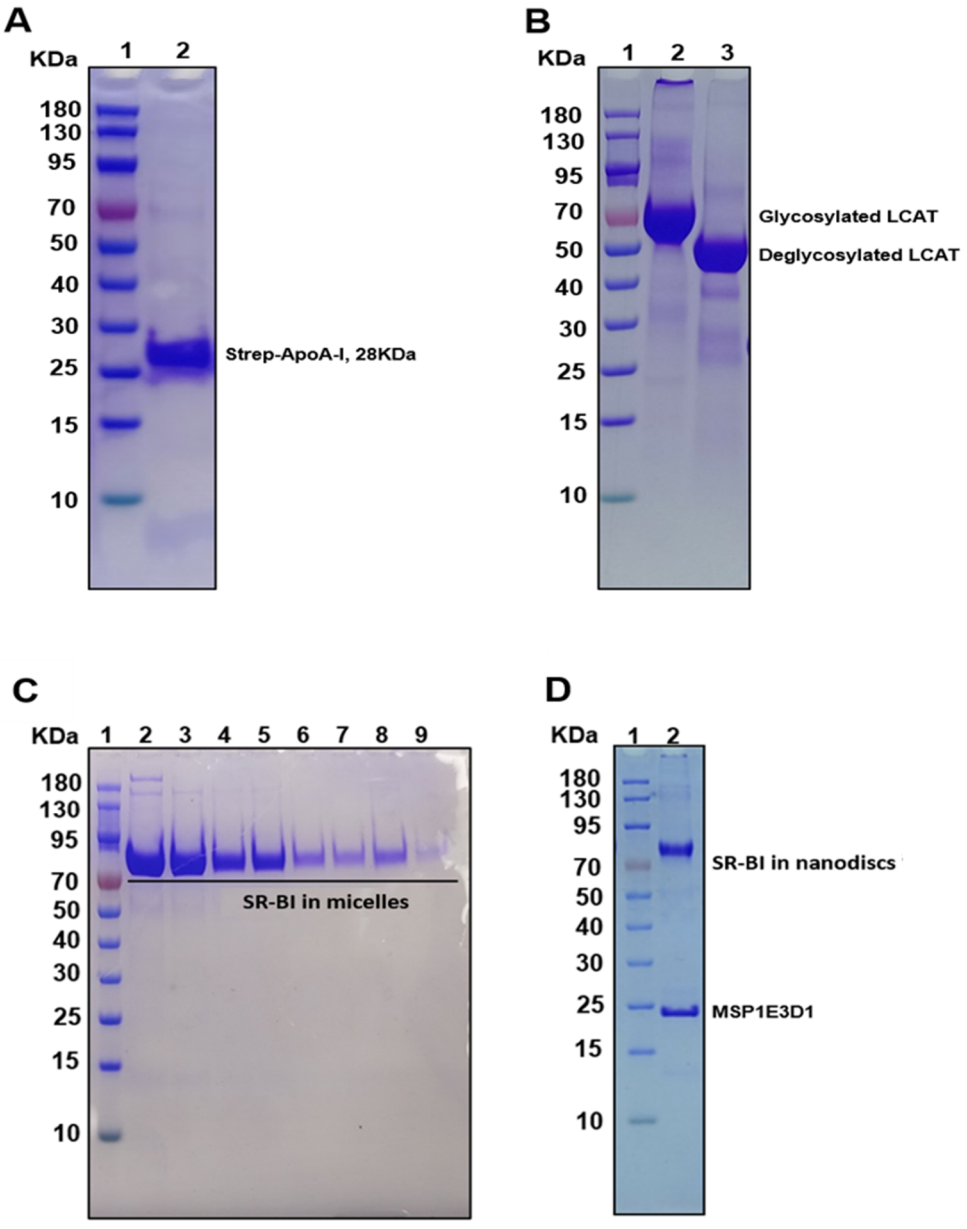
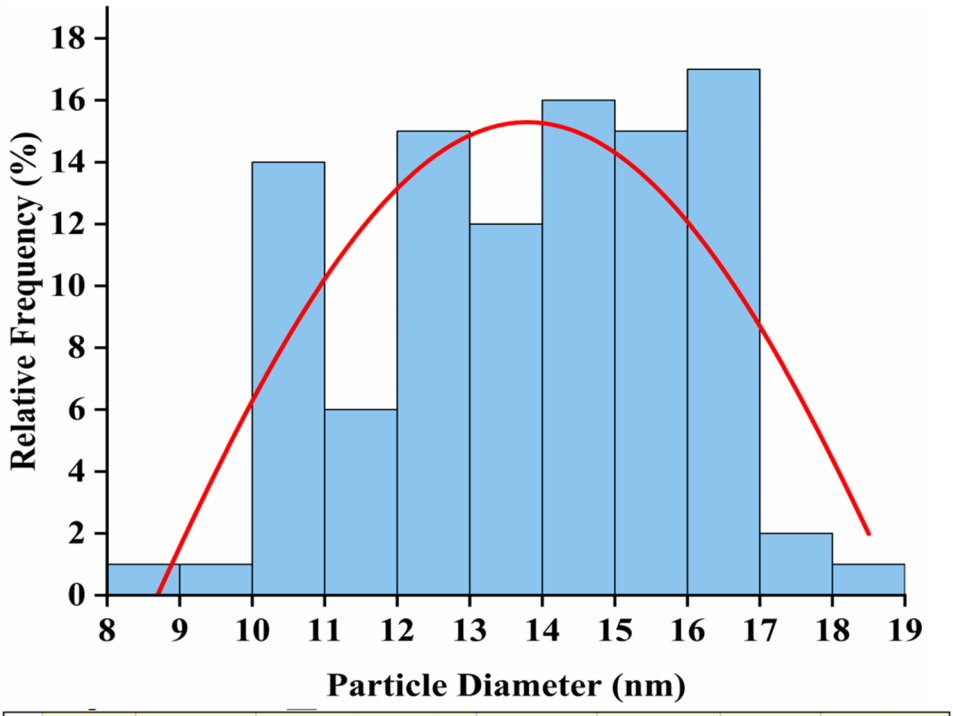


Figure S1. SDS–PAGE analysis of purified Strep-ApoA-I, glycosylated and deglycosylated LCAT and SR-BI samples used for BLI assays. (**A**) Purified Strep-ApoA-I. Lane 1, molecular mass marker; lane 2, purified Strep-ApoA-I. (**B**) Glycosylated and deglycosylated LCAT. Lane 1, molecular mass marker; lane 2, glycosylated LCAT; lane 3, deglycosylated LCAT. (**C**) SEC fractions containing purified SR-BI in micelles. Lane 1, molecular mass marker; lanes 2–9, SR-BI-containing fractions. (**D**) Purified SR-BI reconstituted in nanodiscs. Lane 1, molecular mass marker; lane 2, SR-BI nanodisc sample containing SR-BI (upper band) and MSP1E3D1 (lower band).

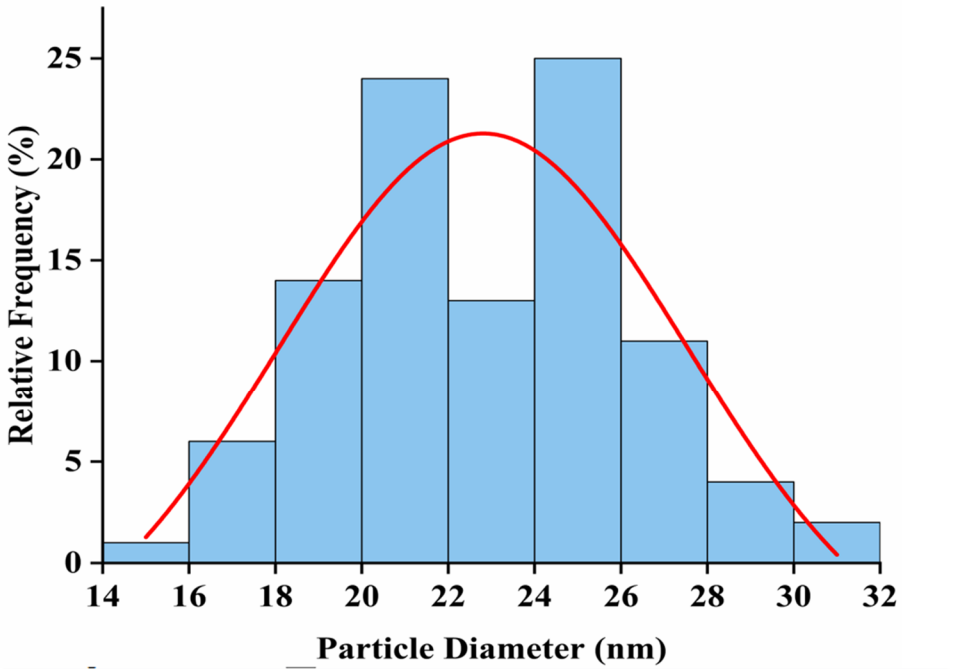
Copyright: © 2026 by the authors. This is an open access article under the terms and conditions of the Creative Commons Attribution (CC BY) license (https://creativecommons.org/licenses/by/4.0/).
Publisher's Note: Scilight stays neutral with regard to jurisdictional claims in published maps and institutional affiliations.

A



	N total	Mean	Standard Deviation	Sum	Minimum	Median	Maximum
A	100	13.82018	2.24479	1382.018	8.163	14.155	18.396

B



	N total	Mean	Standard Deviation	Sum	Minimum	Median	Maximum
A	100	22.88014	3.45164	2288.014	14.268	22.67	30.656

Figure S2. Size distribution of discoidal and LCAT-remodeled spherical-like rHDL particles measured from negative-stain TEM images**.** Blue histograms show the relative frequency distributions of particle diameters, and red curves indicate Gaussian fits to the distribution. (**A**) Discoidal rHDL (d-rHDL), $n = 100$ particles, mean diameter = 13.82 ± 2.23 nm, median = 14.16 nm, range = 8.16–18.40 nm. (**B**) Spherical-like rHDL (s-rHDL), $n = 100$ particles, mean diameter = 22.88 ± 3.45 nm, median = 22.67 nm, range = 14.27–30.66 nm.

Table S1. Chemical shift positions, peak volume, peak height, and linewidths of the 11 selected resonances in the ^{1}H-^{15}N HSQC spectrum of d-rHDL. w1 and w2 denote the peak positions in the ^{15}N and ^{1}H dimensions, respectively. lw1 and lw2 denote the linewidths in the ^{15}N and ^{1}H dimensions, respectively.

Peaks	w1	w2	Volume	Data Height	lw1 (hz)	lw2 (hz)
1	130.395	10.385	1.58×10^{12} ga	8,308,284,928	29.3	54.3
2	129.715	10.106	1.05×10^{12} ga	8,113,623,040	36.9	54.7
3	128.319	7.873	7.34×10^{12} ga	237,559,300,096	30	32.9
4	122.996	8.092	2.43×10^{12} ga	41,595,670,528	24.7	45.2
5	121.829	8.374	1.14×10^{12} ga	13,771,181,056	25.5	75.4
6	121.007	7.896	6.16×10^{11} ga	13,168,101,376	21.2	23.3
7	113.874	7.581	3.32×10^{12} ga	10,848,015,360	33.7	72.9
8	113.855	7.421	3.51×10^{12} ga	15,474,291,712	25.7	44.2
9	111.75	7.47	3.06×10^{11} ga	9,587,633,152	25.6	37.1
10	113.878	6.827	2.83×10^{13} ga	12,640,990,208	51.1	40.8
11	113.611	6.698	1.15×10^{13} ga	36,810,653,696	199.8	48.4

Table S2. Chemical shift positions, peak volume, peak height, and linewidths of the 11 selected resonances in the ^{1}H-^{15}N HSQC spectrum of s-rHDL. w1 and w2 denote the peak positions in the ^{15}N and ^{1}H dimensions, respectively. lw1 and lw2 denote the linewidths in the ^{15}N and ^{1}H dimensions, respectively.

Peaks	w1	w2	Volume	Data Height	lw1 (hz)	lw2 (hz)
1	130.055	10.348	4.51×10^{11} ga	9,180,126,208	34.5	162.6
2	129.666	10.069	5.31×10^{11} ga	8,610,690,048	37.8	104.5
3	128.231	7.882	2.26×10^{12} ga	75,551,072,256	23.9	36.3
4	123.041	8.094	1.34×10^{12} ga	39,894,958,080	30.1	61.1
5	121.833	8.381	7.53×10^{11} ga	7,717,244,928	46.6	95.3
6	121.455	7.905	7.14×10^{10} ga	4,536,044,544	25.2	52.6
7	113.822	7.577	6.35×10^{11} ga	9,068,376,064	40.9	200
8	113.806	7.422	5.20×10^{11} ga	14,117,582,848	37.4	199.9
9	111.827	7.483	1.44×10^{11} ga	4,644,310,016	31.9	28.4
10	113.686	6.84	5.63×10^{11} ga	10,448,197,632	200	200
11	113.605	6.706	4.54×10^{12} ga	19,173,445,632	180.8	65.9